Spin-spin cross relaxation and spin-Hamiltonian spectroscopy by optical pumping of Pr^{3+}:LaF_3

M. Lukac, F. W. Otto, and E. L. Hahn
Department of Physics, University of California, Berkeley, California 94720
(Received 31 August 1988)

We report the observation of an anticrossing in solid-state laser spectroscopy produced by cross relaxation. Spin-spin cross relaxation between the ^{141}Pr- and ^{19}F-spin reservoirs in Pr^{3+}:LaF_3 and its influence on the ^{141}Pr NMR spectrum is detected by means of optical pumping. The technique employed combines optical pumping and hole burning with either external magnetic field sweep or rf resonance saturation in order to produce slow transient changes in resonant laser transmission. At a certain value of the external Zeeman field, where the energy-level splittings of Pr and F spins match, a level repulsion and discontinuity of the Pr^{3+} NMR lines is observed. This effect is interpreted as the "anticrossing" of the combined Pr-F spin-spin reservoir energy states. The Zeeman-quadrupole-Hamiltonian spectrum of the hyperfine optical ground states of Pr^{3+}:LaF_3 is mapped out over a wide range of Zeeman magnetic fields. A new scheme is proposed for dynamic polarization of nuclei by means of optical pumping, based on resonant cross relaxation between rare spins and spin reservoirs.

I. INTRODUCTION

Several methods for the sensitive detection of the magnetic resonance of hyperfine-coupled states of optically resonant ions by laser excitation in solids have been reported.[1-4] In this paper we describe a special optical pumping method[5] which makes possible extended measurements of complicated hyperfine spectra. The Zeeman-split ground-state hyperfine-level spectroscopy of quadrupole coupled Pr^{3+} in its lowest electronic crystal-field state is determined over a wide range of magnetic fields in a single crystal of Pr^{3+}:LaF_3. Measurements of the effects of cross relaxation and level crossing between rare Pr^{3+} spins and abundant F spins are also carried out. During optical pumping the technique requires that spin transitions must be imposed at optimum rates that first increase and then decrease in non-equilibrium over short time periods. As a result, transient reductions in laser transmission (increased absorption) take place which signify that spin transients have occurred.

In the optical pumping cycle, resonant laser light excites the Pr^{3+} system from given ground states to excited states. From these states the fluorescence decay process transforms the system to final states different from the initial states. Some degree of hole burning[1] occurs if the pump intensity is sufficient to overcome the rate at which spin-lattice relaxation and other coupling mechanisms among the Pr^{3+} hyperfine states restore the original ground-state population distribution. When the transmitted laser pump intensity is first adjusted to an optimum steady-state value, any nonequilibrium change in the populations of the Pr^{3+} ground states produces a sudden increase in laser-beam absorption. The optical transmission undergoes an incoherent transient reduction and then recovers toward the previous steady state. "Sudden" change here does not mean that coherent transients take place. Instead the Pr^{3+} spin population changes occur on a time scale short compared to the time required for the system to approach equilibrium, but long compared to the lifetimes of coherent transients.

Attempts to detect alterations of hyperfine state distributions by steady-state radio frequency (rf) saturation result in only very small reductions in laser transmission, revealed at best when hyperfine states are degenerate in zero magnetic field, and when spin-lattice relaxation times T_1 are short. Over a wide range of magnetic fields $B > 100$ G, with T_1 times much longer, this steady-state procedure is useless for data taking because noise amplitude fluctuations proportional to $1/f$ (at low frequencies f) in the laser-beam frequency and intensity obscure the final dc signal which is to be measured after integration. For this reason a time varying method of rf saturation is used where spin transitions are imposed suddenly but incoherently at a convenient repetition rate. This nonequilibrium method has no counterpart in previous optical experiments in solids, and provides flexibility in the detection of hyperfine-level transitions over a wide range of Zeeman-split hyperfine levels.

Zeeman-level spectroscopy is carried out by the application of bursts of rf fields (for a given value of B) at resonance between hyperfine states over a wide range of Zeeman splittings. In our observations all detected splittings are greater than the spectral width of the laser which is about 1 MHz. Another means of imposing sudden spin transitions among pairs of Pr^{3+} levels is to produce Zeeman-field sweeps over critical values of B which match Pr^{3+} level pair transitions with the Zeeman splitting of neighboring F nuclear moments. The cross relaxation which results has an effect similar to that of external rf saturation of the Pr^{3+} levels. These level-crossing conditions together with the rf saturation data help to confirm the correct Zeeman quadrupole spectrum of the

ground-state Pr^{3+} levels.

Our study of the enhanced Pr nuclear Zeeman gyromagnetic tensor in the Pr^{3+}:LaF_3 system shows that the published fit[6] to previously obtained low-magnetic-field data is not unique. The correct analysis of the nuclear quadrupole and Zeeman coupling tensors can only be made at higher values of the B field where the Zeeman interaction becomes comparable to the nuclear quadrupole interaction. When Pr- and F-spin levels nearly match in constant Zeeman field, a slight repulsion of the level pairs is observed, not to be confused with level crossings[7] among levels of the same spin. This observation is made from changes in optical pumping which result from bursts of rf NMR saturation fields applied at a resonance transition between a third Pr level and one of the pair of Pr levels which cross or matches the spin transition of neighboring F nuclear moments. Therefore, as a function of the B field, the eigenfrequency of a particular Pr level can be followed as it passes through the cross-relaxation matching condition, showing a level repulsion "kink." This discontinuity in the Pr spectrum resembles the effect of an off-resonance Pake doublet[8] for $I=\frac{1}{2}$. Assume for simplicity that two different spins, labeled by different gyromagnetic ratios γ_1 and γ_2, are dipolar coupled. While γ_2 is held fixed suppose γ_1 is adjustable (which provides the same effect as adjusting the magnetic field B), and approaches the value of γ_2. As γ_1 passes through the value of γ_2, mutual spin flips occur which produce an additional "coherent splitting" superimposed on the static splitting always present due to the diagonal term of the dipole-dipole interaction. In reality a single Pr spin is coupled to a cluster of near F neighbors which in turn couples to the large F-spin reservoir. This represents a more complicated cross-relaxation mechanism, and yet level repulsion is observed in spite of the obscuring effect of dipolar broadening.

Conventional[9,10] nuclear-spin cross-relaxation measurements which measure spin population differences directly, whether by double resonance methods or by direct laboratory Zeeman-field level crossing, do not reveal the level-crossing effect. At the onset of cross relaxation a resonant transfer of spin magnetization is monitored only when the levels match; no spectroscopy of the level splittings is visible above or below the matching frequency. In the optical pumping method the response is proportional to the absolute population of a given spin hyperfine level rather than to population level differences, which allows the eigenlevels to be tracked throughout the region of the matching condition. We note that in a previous investigation[11] a similar method has been applied to the study of organic solids.

II. Pr^{3+}:LaF_3 HAMILTONIAN AND CRYSTAL STRUCTURE

The inhomogeneously broadened $^3H_4(\Gamma_1)\leftrightarrow{}^1D_2(\Gamma_1)$ ($\lambda=592.5$ nm) optical transition[12] of Pr^{3+} with spin $I=\frac{5}{2}$ has three nuclear-spin ground-state levels present in zero magnetic field ($B=0$) with separations in frequency[1,3] determined by the enhanced[13] nuclear-quadrupole interaction. For $B\neq 0$ each of these levels is split into two levels by the enhanced Zeeman interaction as shown in Fig. 1. Similarly, split nuclear quadrupole levels exist in the excited $^1D_2$ optical state but they do not play a role in our measurements. The six possible levels in the excited state are assumed to be equivalent and are lumped together in the phenomenological treatment which follows later.

The Hamiltonian of this system is characterized by Teplov[13] as follows:

$$\mathcal{H}_{Pr}=-\hbar(\gamma_x^{Pr}B_xI_x+\gamma_y^{Pr}B_yI_y+\gamma_z^{Pr}B_zI_z)+D\left[I_z^2+\frac{I(I+1)}{3}\right]+E(I_x^2-I_y^2)\ , \tag{1}$$

where $D/h=4.1797\pm0.0013$ MHz and $E/h=0.154\pm0.004$ Mhz.[3] The enhanced nuclear Zeeman tensor γ^{Pr} is

$$\gamma_i/2\pi\ (\text{kHz/G})=\frac{(g_N\mu_N+2g\mu\Lambda_{ii})}{h}\ .$$

Here μ_N and μ are the nuclear and electron Bohr magneton, respectively, g_N and g are the nuclear and electron splitting g factor, respectively, and

$$\Lambda_{ii}=\sum_{n\neq 0}\frac{A_i|\langle 0|J_i|n\rangle|^2}{E_n-E_0}\ .$$

The gyromagnetic enhancement parameter Λ_{ii} is determined by the coupling of the angular momentum J_i between ground- and higher-angular-momentum states of Pr^{3+}, characterized by energies E_0 and E_n, respectively, with $i=x,y,z$ and A_j is the hyperfine coupling constant.

The Zeeman Hamiltonian for the fluorine spins ($S=\frac{1}{2}$) in a magnetic field is

$$\mathcal{H}_F=-\hbar\gamma^F\sum_i B_iS_i\ , \tag{2}$$

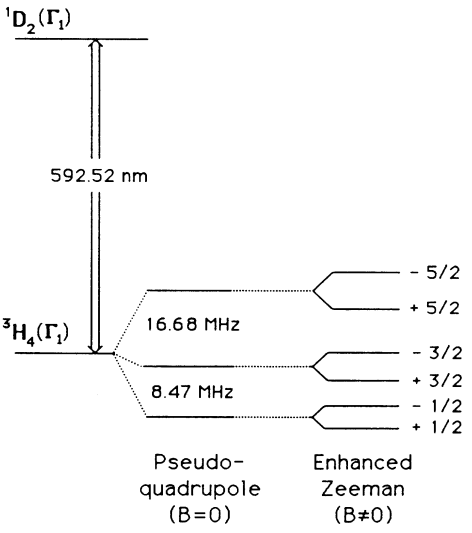

FIG. 1. The optical ground-state splittings of Pr^{3+}:LaF_3.

where $i=x,y,z$ and $\gamma^F=4.0055$ kHz/G. The dipole-dipole coupling between F and Pr accounts for a spin resonance width among any of the Pr transitions of about 100 kHz.

The crystal structure of LaF_3, showing only the La ion positions, is depicted in Fig. 2.[14] At the crystal sites where Pr^{3+} substitutes for La^{3+} there are three pairs of symmetry axes oriented at 120° with respect to each other in the plane perpendicular to the C_3 axis. Each Pr^{3+} ion is surrounded by neighboring fluorine ions in such a way that the site axis has at least a twofold symmetry (C_2). Because the optical electric dipole transition can be excited only by a laser electric field $\mathbf{E}_L$ which has a component along a crystal C_2 axis, it is possible to excite selectively different sets of inequivalent crystal sites by choosing the proper exciting laser polarization.

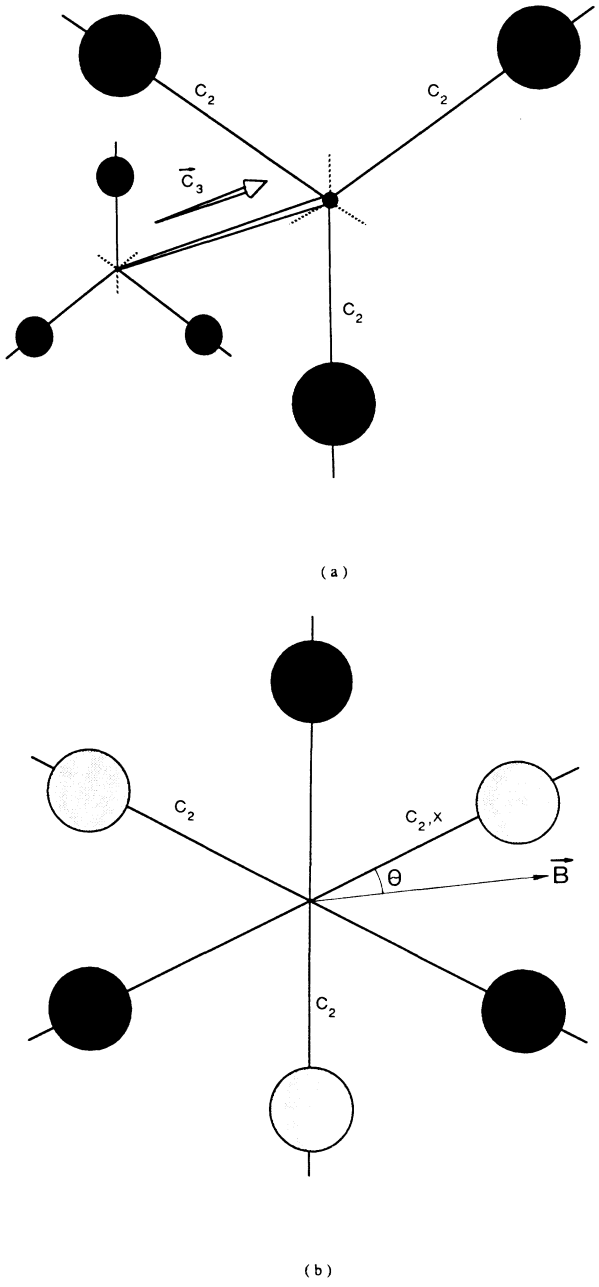

FIG. 2. Part of the crystal structure of LaF_3. (a) Perspective view (not to scale). The angle between the quadrupole-tensor z axis and the C_3 axis is 91.4° and the x axis coincides with the C_2 axis. (b) View along the C_3 axis; θ is the angle between the applied magnetic field B and the local-quadrupole x axis (a C_2 axis).

III. TEMPORAL LASER-BEAM ABSORPTION

A number of simplifying assumptions will be made in order to develop a set of rate equations describing optical pumping combined with simultaneous resonance transitions among hyperfine levels in the optical ground state. The laser is resonant with the main optical ${}^3H_4(\Gamma_1)\leftrightarrow{}^1D_2(\Gamma_1)$ transition at $\lambda=592.5$ nm. The measurements are made for Zeeman hyperfine splittings greater than the 1 Mhz spectral linewidth of the CW laser. The splittings among the six hyperfine excited-state levels play no significant role in our measurements because the fluorescence lifetime $T_f=0.5$ msec (Ref. 12) is much shorter than any relaxation time among these levels. Therefore we assume these excited levels are equivalent and are not coupled to one another. The optical transition displays a Stark-strain-field linewidth of approximately 10 GHz. Within the laser spectral width of 1 MHz the laser excites about $10^{-4}N$ Pr^{3+} ions, where $N\approx10^{19}$ ions/cm^3 for a 0.5 at. % doped single LaF_3 crystal used in our experiment. For different ions in the inhomogeneous line a two-level optical transition can take place from any one of the six Zeeman-split ground-state hyperfine levels to any one of the six excited-state levels. The rate of laser excitation W_L (sec^{-1}) is assumed to be equal for each transition.

Because of the inhomogeneous broadening of the optical line there are six sets of optically excited ions corresponding to the six different ground-state levels of the Pr ions in a nonzero magnetic field which can be in resonance with the laser excitation. (In zero magnetic field, there are only three sets corresponding to the three doubly degenerate ground-state levels.) Let us assume that a magnetic-resonance transition takes place between a pair of hyperfine ground-state levels α and β, where $E_\beta>E_\alpha$. This transition can be incurred either by externally excited resonance or by level crossing with neighboring fluorine nuclei. Either of these mechanisms is denoted for simplicity by the rate W_C (sec^{-1}). Later the use of rate parameter W_c must be modified for certain conditions of level crossing. The other four Pr^{3+} ground-state levels are denoted by σ. For the analysis in this section, we collect the six sets of Pr^{3+} ions into three distinct groups (see Fig. 3). Those ions which have level α resonant with the laser excitation are in group A, while those ions excited from level β are in group B. The other four sets of ions excited by the laser are in group C. In developing the rate equations which follow we consider only the two groups of ions A and B, since the optical pumping cycle of group C is not affected by the magnetic-resonance excitation.

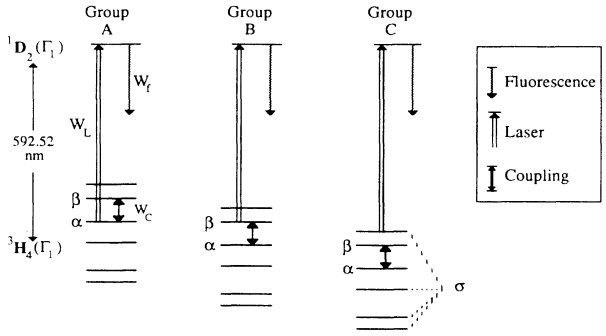

FIG. 3. Three groups of Pr^{3+} ions depending on which of the ground-state hyperfine levels is in resonance with the optical excitation.

We describe the ground-state spin-level populations of groups A and B by the combined populations n_1 n_2, and n_3. The two coupled ground-state levels α and β are represented by populations n_1 and n_2, where n_1 represents the population of the ground-state level which is resonant with the laser excitation. Note that for group A the populations of levels α and β contribute to levels 1 and 2, respectively, while for group B the populations of levels α and β contribute to levels 2 and 1, respectively. Therefore, for different ions in the inhomogeneous line the energy of level 1 can be either greater or smaller than that of level 2. The remaining ground state populations of levels σ are defined by n_3, having a weight of four in nonzero magnetic field. The spin-lattice relaxation rates for the ground-state hyperfine transitions have been measured only in zero magnetic field.[15] In our analysis we assume for simplicity that the relaxation rates are the same among all the levels and are given by $W_{sl}=1/(2T_1)$.

Since we assume that the excited-state levels are not coupled, there is only one excited state level of interest for each excited ion. We denote the population of the excited state levels by n_4, where n_4 can represent any of the six excited hyperfine levels, depending on the position of the ion within the inhomogeneous optical line. Also, thermal equilibrium polarization is assumed to be zero, relative to large local population differences produced by optical pumping. The rate equations for nonzero magnetic fields are written as follows:

$$\frac{dn_1}{dt}=W_L(n_4-n_1)+W_C(n_2-n_1)+\frac{n_4}{6T_f}+W_{sl}[(n_2+n_3)-5n_1]\ , \tag{3a}$$

$$\frac{dn_2}{dt}=W_C(n_1-n_2)+\frac{n_4}{6T_f}+W_{sl}[(n_1+n_3)-5n_2]\ , \tag{3b}$$

$$\frac{dn_3}{dt}=\frac{4n_4}{6T_f}+W_{sl}[4(n_1+n_2)-2n_3]\ , \tag{3c}$$

$$\frac{dn_4}{dt}=W_L(n_1-n_4)-\frac{n_4}{T_f}\ , \tag{3d}$$

and

$$\sum_i n_i=1\ . \tag{3e}$$

When the initially unperturbed system is allowed to reach equilibrium during a constant optical pumping rate W_L in the absence of magnetic transitions ($W_C=0$), the n_1 level is bleached ($n_1\rightarrow 0$) for $W_L/W_{sl}\gg 1$ and $W_L T_f\gg 1$ (the values of these parameters will be discussed later). The entire ground-state population is now contained in levels n_2 and n_3 [see Fig. 4(a)] which results in an absorption hole in the inhomogeneous optical line. Analysis of Eqs. (3) show (not produced here) that if W_C is then turned on at time $t=0$, a rapid, an almost linear increase in laser-beam absorption occurs for a time $\Delta t\approx 1/W_C$ for $W_C\gg W_L$ until the level pair saturates, and $n_1\approx n_2$. Figure 4(b) depicts a case where the rate W_C is induced by the Pr-F cross relaxation. After the time Δt the laser absorption reaches a maximum, and then declines more slowly as the laser-beam pumps more particles from one of the saturated level pairs (n_α or n_β) until they both empty while W_C maintains $n_1=n_2$ and the fluorescence mechanism $1/T_f$ takes over to fill up the remaining n_3 spin states. Therefore with $W_c\neq 0$ the system reaches new equilibrium with two out of six ground-state levels now empty for $W_C/W_{sl}\gg 1$ [see Fig. 4(c)], and the state of the laser transmission is as it would be with $W_C=0$. The coupling rate W_C is determined either by the strength of the magnetic dipole-dipole interaction among the spins in the case of cross relaxation, or by the strength of the applied field in the case of external rf excitation.

A resonance process in the steady state which renders W_C finite does not necessarily produce useful laser ab-

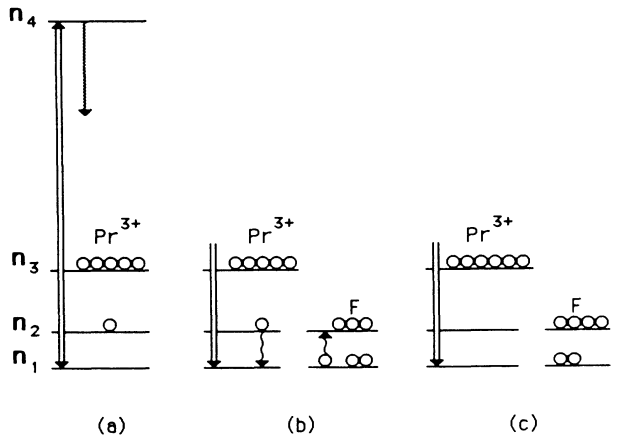

FIG. 4. Temporal optical pumping process. The four levels not participating in the cross relaxation with neighboring fluorines are represented by n_3. In this diagram: (a) optical pumping empties levels n_1; (b) when level crossing occurs, mutual spin flips between Pr and F nuclei empty level n_2; (c) both the n_1 and n_2 levels are empty and the neighboring fluorine nuclei have been partially polarized.

sorption signals to carry out spectroscopy. An observable steady-state decrease in optical transmission because of rf hyperfine transitions could only be observed in magnetic fields smaller than 50 G, where the transmission decreased by as much as 30%. This occurs mainly because the spin-lattice relaxation rate, $W_{sl} \approx 1$ sec^{-1}, is fast enough to overcome the rate of depopulation of the rf coupled hyperfine levels due to optical pumping. For B fields larger than the local dipolar fields the absorption hole lifetime was measured to be on the order of minutes, which implies a slow spin-lattice relaxation rate $W_{sl} < 0.1$ sec^{-1}. In addition, the hyperfine ground states are Zeeman split in nonzero magnetic fields so that only two out of six levels rather than two out of three levels are affected by the rf saturation. For these reasons, the steady-state change of transmission in magnetic fields $B > 50$ G is so small that the amplitude and frequency noise of the laser makes direct absorption measurements impractical; only short-lived changes in optical transmission are observed when rf hyperfine-resonance excitation is turned on. Similarly, tuning the external magnetic field to a level-crossing region does not produce a measurable signal. In order to induce transient changes in Pr hyperfine-level distributions, an externally applied dc magnetic field is swept at an optimum rate through values where the energy difference between two of the Pr ground-state hyperfine levels (denoted by α and β) matches the fluorine spin Zeeman energy difference. During the field sweep the Hamiltonian is changing monotonically. This variation is interrupted near the values of magnetic field where the energy conservation for spin-spin coupling is satisfied and sharp laser absorption peaks are observed.

The dynamics of the cross relaxation of optically pumped Pr spins with the neighboring fluorine spins is very complex, and to solve this problem would be a formidable task. The Pr-F cross-relaxation process is complicated even more when the level crossing in our experiment is induced by the external magnetic sweep. Either of the limits of rapid or slow spin-flip diffusion among the fluorine spins may be applied to describe the effect of level crossing on the laser-beam transmission. These correspond to spin-spin relaxation inequalities T_2 (F-F) $\geq T_2$(Pr-F) for the slow limit and T_2(F-F) $< T_2$(Pr-F) for the fast limit. In the Appendix we discuss the diffusion limited case and we show that a range of parameters in our experiment can foster a diffusion bottleneck. The role of spin diffusion suggested by our experiment could be of significance in other systems which are governed by the types of interactions included in Eqs. (3). In our experiments which mainly confirm spectral values, the requirement of B field and rf sweep variations to obtain Pr spin resonance imposes complicated initial conditions. Our data are insufficient to confirm the existence of any degree of F-F spin-flip diffusion bottleneck. In what follows we assume the fast diffusion limit where the use of W_C as it stands in Eq. (3) is valid. In this case the F spin ensemble is coupled to an equal extent with both positively and negatively oriented Pr spins during the process of optical pumping. The Pr level pairs are therefore in contact with a completely depolarized F-spin reservoir defined at infinite spin temperature. It is shown in the Appendix that the cross coupling rate W_C between the Pr and F spins can be expressed in a form

$$W_C = W_0 \exp\left[-\frac{(\omega_{Pr} - \omega_F)^2}{2\langle \Delta\omega^2 \rangle} \right] . \tag{4}$$

The exponential term in Eq. (4) is the level-crossing tuning parameter, where $\langle \Delta\omega^2 \rangle = (\langle \Delta\omega_{Pr}^2 \rangle + \langle \Delta\omega_{FF}^2 \rangle)$, and $\langle \Delta\omega_{FF}^2 \rangle$ and $\langle \Delta\omega_{FF}^2 \rangle$ are, respectively, the second moments of the Pr- and F-spin lines. The strength of the coupling at exact resonance ($\omega_{Pr} = \omega_F$) is estimated to be $W_0 \approx |M|^2 \times 10^6$ sec^{-1}, where

$$|M|^2 = |\langle E_{Pr}, E_F | I_+^{Pr} S_-^{Fi} + I_-^{Pr} S_+^{Fi} | E_{Pr} \pm \hbar\omega_{Pr}, E_F \mp \hbar\omega_F \rangle|^2 . \tag{5}$$

The exact value of $|M|^2$ depends on the degree to which Pr-spin eigenvectors are mixed to allow $\Delta m = \pm 1$ transitions, and the maximum possible value of $|M|^2$ being on the order of unity. In the Appendix we also show that the cross coupling can be diffusion limited for coupling strengths $W_C \geq 10^4$ sec^{-1}.

The width of the cross-relaxation response in terms of the change in the applied magnetic field B is determined by the difference in slopes at which the eigentransitions of the F and Pr spins intersect. The coupling rate expressed in terms of the external magnetic field is

$$W_C = W_0 \exp\left[-\frac{(B - B_r)^2}{2(\delta_B)^2} \right] , \tag{6}$$

where B_r is the resonant value of the magnetic field where Pr- and F-spin lines match, and $\delta_B = \langle \Delta\omega^2 \rangle^{1/2} [d(\omega_{Pr} - \omega_F)/dB]^{-1}$. If we take $\langle \Delta\omega^2 \rangle^{1/2} /(2\pi)$ to be 100 kHz and take a typical value of $(1/2\pi)[d(\omega_{Pr} - \omega_F)/dB]$ from our data of 4 kHz/G, we obtain an approximate width of $\delta_B \approx 25$ G.

During the magnetic field sweep, the optical transition frequencies of the Pr^{3+} ions are constantly changing because of the Zeeman effect on both the ground- and excited-state energy eigenlevels. As shown in Fig. 5, ions which were previously resonant with the laser are constantly being swept out of resonance while fresh ions are coming into resonance. Neglecting the small Zeeman broadening in the 10 GHz width of the optical line, the number of ions that are resonant with the laser remains constant. The spin temperature of the Pr ions coming into resonance is that of the surrounding lattice, while those spins moving out of resonance have had their level populations redistributed by the optical pumping. This magnetic field sweep effect is incorporated into a simplified model by describing it in terms of an average rate W_B (sec^{-1}) proportional to dB/dt. Since ions are transferred into and out of optical resonance, we assume that the total number of ions at resonance, n_0, is conserved. For the Pr spins which have not been in resonance with the laser, the high-temperature approximation applies at 2 K and the ground-state spin levels are equally populated. The spin-level populations of the optically resonant ions change because of the magnetic field

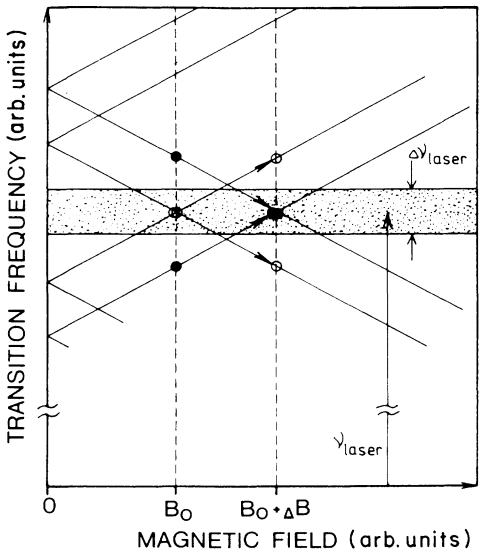

FIG. 5. Effect of magnetic-field sweep on optical excitation, assuming for simplicity that quadrupole levels vary linearly, with equal density of states increasing and decreasing in energy as a function of B. A narrow laser with a linewidth of $\Delta\nu_{laser}\approx 1$ MHz excites only a fraction of Pr^{3+} ions in the 10-GHz inhomogeneously broadened $^3H_4\leftrightarrow{}^1D_2$ optical line. If the external magnetic field is held fixed, these resonant ions are polarized by optical pumping. When the external field B is changed by ΔB, the transition frequencies of the Pr^{3+} ions change due to the nuclear Zeeman effect, causing the previously resonant ions (represented by open circles) to move out of the optical resonance. At the same time some of the previously nonresonant ions (represented by solid circles) become resonant with the laser excitation.

sweep according to the following rate equations [which are independent of the other rate processes, and are added later to Eqs. (3)]

$$\frac{dn_1}{dt}=-W_B n_1+\frac{W_B n_0}{6}\ , \tag{7a}$$

$$\frac{dn_2}{dt}=-W_B n_2+\frac{W_B n_0}{6}\ , \tag{7b}$$

$$\frac{dn_3}{dt}=-W_B n_3+\frac{4W_B n_0}{6}\ , \tag{7c}$$

and

$$\frac{dn_4}{dt}=-W_B n_4\ , \tag{7d}$$

where

$$n_0=\sum_i n_i\equiv 1\ . \tag{7e}$$

We assume that the excited-state population of off resonant ions is zero. Because of the complexity of the many lines involved with inhomogeneous broadening, we also assume that the six ground levels are swept into resonance at the same average rate (with n_3 again given a weight of four). Note that the excited n_4 levels do not display polarization in our model.

From our original assumption we define the proportionality constant χ by

$$\frac{dB}{dt}=\chi W_B\ . \tag{8}$$

A typical rate of change of the Pr^{3+} optical transition frequencies versus magnetic field due to the enhanced Zeeman effect is 4 kHz/G. Therefore Pr^{3+} ions remain in resonance with the laser (with a spectral width of 1 MHz) only for a time

$$\delta t=(1\ \text{MHz})/[(4\ \text{kHz/G})(dB/dt)]\ .$$

This implies that the rate at which ions are swept in and out of resonance with the laser is $W_B=\delta t^{-1}$, and thus χ is approximately 250 G.

When we add the terms of Eqs. (7) to those of Eqs. (3), we arrive at a complete set of five coupled equations which describe the entire process, incorporating optical pumping, field sweep, and cross-relaxation processes

$$\frac{dn_1}{dt}=W_L(n_4-n_1)+W_C(n_2-n_1)+\frac{n_4}{6T_f}+W_{sl}[(n_2+n_3)-5n_1]-W_B n_1+\frac{W_B}{6}\ , \tag{9a}$$

$$\frac{dn_2}{dt}=W_C(n_1-n_2)+\frac{n_4}{6T_f}+W_{sl}[(n_1+n_3)-5n_2]-W_B n_2+\frac{W_B}{6}\ , \tag{9b}$$

$$\frac{dn_3}{dt}=\frac{4n_4}{6T_f}+W_{sl}[4(n_1+n_2)-2n_3]-W_B n_3+\frac{4W_B}{6}\ , \tag{9c}$$

$$\frac{dn_4}{dt}=W_L(n_1-n_4)-\frac{n_4}{T_f}-W_B n_4\ , \tag{9d}$$

and

$$\sum_i n_i\equiv 1\ . \tag{9e}$$

The time evolution of the optical transmission when the magnetic field is swept across the cross-relaxation region is calculated in the following way: Steady-state solutions to Eqs. (9), calculated in a region where $W_C=0$, are used as the initial values for the level populations n_i. The initial value of the magnetic field is fixed in a region where W_C is negligible, 150 G below the cross-relaxation resonance. The level populations n_i as a function of time are then obtained by solving Eqs. (9) numerically, where W_C is a function of the external magnetic field B according to Eq. (6), and B is varied in time according to Eq. (8), and the following values are used: $\delta_B=10$ G, $\chi=250$ G, the maximum coupling rate $W_0=100\ \text{sec}^{-1}$, the spin-lattice relaxation rate $W_{sl}=0.1\ \text{sec}^{-1}$, and $T_f=5\times10^{-4}$ sec.

Some results of the calculations expressed in terms of transmission are shown in Fig. 6. It is assumed that the transmission T is given by

$$T=\frac{I_{\text{in}}}{I_{\text{out}}}=\exp[-kL(n_1-n_4)]\ , \tag{10}$$

where I_{in}, and I_{out} are the input and output light intensities, L is the length of the sample, and k is the absorption coefficient. The product kL is determined by the low-intensity steady-state transmission, which was measured to be $T\approx 20\%$, giving $kL\approx 0.3$ for $n_1=\frac{1}{6}$, and $n_4=0$.

As discussed above, the magnetic-field sweep is applied in order to produce transient changes in the hole-burning processes. However, the field sweep also prevents complete hole burning because of the constant exchange of resonant ions, reducing the sensitivity of the measurement. Figure 6(a) illustrates that there is an optimal rate for dB/dt. In a fast sweep, when dB/dt (and hence W_B) is too large, there is no hole burning, while during a slow sweep the onset of spin-spin coupling is too gradual to be observed. Similarly, Fig. 6(b) shows that there is an optimum value for the optical pumping rate W_L. When the pumping is too weak there is no hole burning and when it is too strong the coupling between levels is too small a perturbation to be detected. This dependence on W_L applies also in the case where the magnetic field is held constant and the coupling W_C is caused by a sudden application of resonant rf. It should be noted that the optimum values of W_L and W_B depend also on the strength of the coupling W_c.

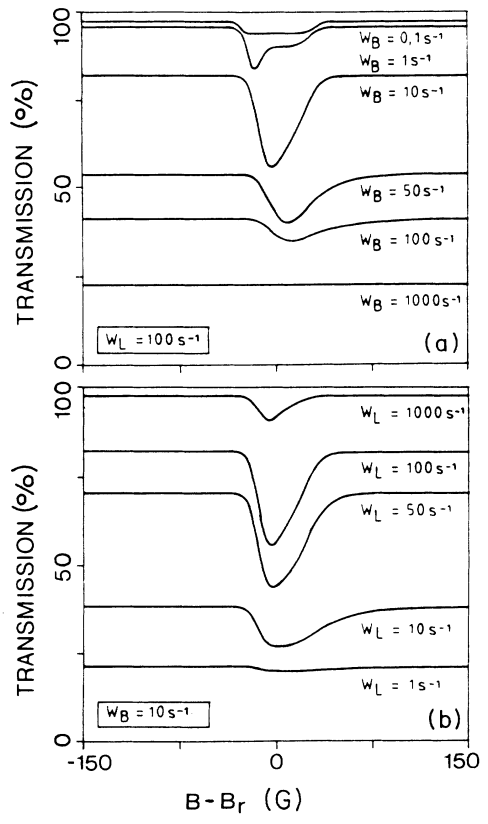

FIG. 6. Calculated time evolution of the optical transmission when the magnetic field is swept at a rate dB/dt across the Pr-F–spin cross-relaxation point B_r. (a) Dependence of the transmission resonance on the magnetic-field sweep rate ($dB/dt = W_B \times 250$ G) at a constant optical pumping rate of $W_L = 100$ sec^{-1}. (b) Dependence of the transmission resonance on the optical pumping rate W_L at a constant magnetic-field sweep rate of $W_B = 10$ sec^{-1}. A rate of $W_L = 100$ sec^{-1} corresponds approximately to a laser intensity of 20 mW/mm^2.

The experiment confirms a very sensitive dependence of signal strength on the sweep rate and laser intensity. In fact, unless special care is taken in choosing the proper experimental parameters no effect can be seen. When the magnetic-field sweep rate is reduced from an optimum value of 500 G/sec ($W_B = 2$ sec^{-1}) to 200 G/sec, previously visible changes in laser transmission can no longer be seen. Similarly, an increase in the sweep rate to 800 G/sec reduces detection sensitivity by a factor of 2. As is the case with the sweep rate, the signal is also reduced if the laser intensity is higher or lower than the optimum intensity of about 20 mW/cm^2. In a separate experiment where steady-state transmission versus laser intensity was measured, we determined that 20 mW/cm^2 corresponds to $W_L \approx 100$ sec^{-1}. Despite the crudeness of our model, these empirically determined optimal parameters are in good agreement with the rate equation model. The model also shows that the absorption peaks do not necessarily occur exactly at resonant values of B_r, but can appear shifted below or above resonance depending on the experimental parameters used. This error can be estimated and compensated for by performing magnetic-field sweeps in both directions.

IV. rf SPECTROSCOPY RESULTS

A 0.1 at.% Pr^{3+}:LaF_3 crystal with dimensions of $3\times3\times7$ mm^3 was immersed in liquid helium inside an rf coil and cooled to 1.8 K. The crystal was aligned so that its C_3 axis was parallel to the coil axis and perpendicular to the applied magnetic field, **B**. In addition, one of the crystal C_2 axes was aligned approximately parallel to the magnetic field. The laser pump was provided by a Coherent Model 599/21 frequency-stabilized cw dye laser source which was linearly polarized. The laser linewidth was 1-MHz rms and the incident light intensity at the sample was 20 mW/cm^2. An rf field of approximately 1 G was applied for 0.5 sec, which was the duration of the transient transmission decrease. Optical transmission was monitored by a *p-i-n* photodiode, ac coupled to a gated integrator with output connected to a chart recorder (see Fig. 7). The rf field was applied empirically at a repetition rate of one pulse every seven seconds to optimize the integrated optical-transient signal. Waiting for longer times decreased the amount of data collected and did not significantly improve the signal-to-noise ratio. Although the recovery time between pulses was considerably less than the effective nuclear T_1, sufficient population was recovered in this short time to produce a usable signal. By shifting the rf frequency between each pulse and keeping the external magnetic field fixed, it was possible to map out some of the NMR transitions. The magnetic field was then changed and the process repeated to

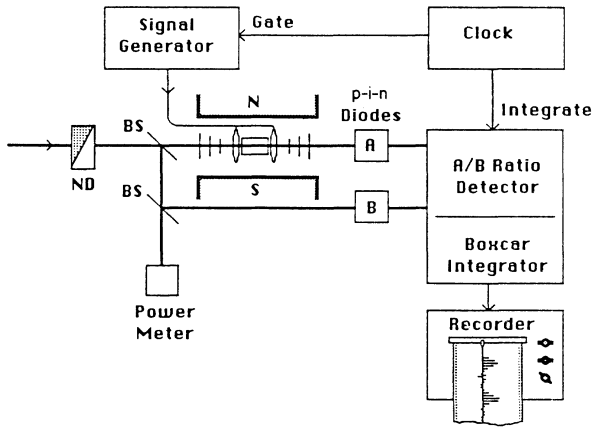

FIG. 7. Experimental apparatus for the rf spectroscopy experiment. rf pulses ($H_1 = 1$ G) were applied and changes in optical transmission noted. BS is the beam splitter; ND is the neutral density wedge.

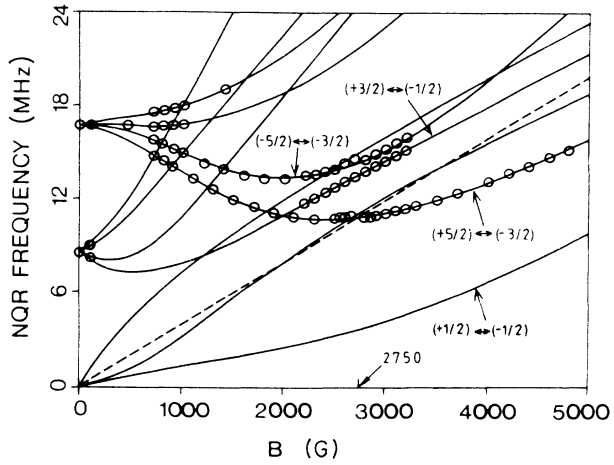

FIG. 8. The rf data (circles) and numerical fit (solid line) to the Pr-spin Hamiltonian for $\theta = 1.5°$, $\gamma_x^{Pr}/2\pi = 3.45$ kHz/G, $\gamma_y^{Pr}/2\pi = 4.98$ kHz/G, and $\gamma_z^{Pr}/2\pi = 10.16$ kHz/G. The dashed line is the fluorine transition. The arrow at $B = 2750$ G indicates the Pr-$|+\frac{5}{2}\rangle \leftrightarrow |-\frac{3}{2}\rangle$ and F-line crossing.

obtain sufficient rf data to fit the theory to within ± 100 kHz. The results which follow depend upon the state mixing in a magnetic field caused by both the Zeeman and quadrupole interactions. This mixing allows transitions between any two states to occur. Attempts to obtain signals for transitions with frequencies below 6 MHz were unsuccessful. This is thought to be due to laser-frequency fluctuations which cause the closely spaced ground-state levels to be pumped nonselectively. There is also the possibility of cross relaxation with nearby fluorine and lanthanum nuclei ($I = \frac{7}{2}$). Both of these nuclei have splittings of less than 6 MHz for fields below 1500 G where the measurements were done. As several strong lines were followed to higher magnetic fields the signal decreased until they eventually became too weak to detect. At high fields the states become more pure and with less state mixing the required optical pumping to levels with differing nuclear m_I is decreased. In particular, the $|+1/2\rangle \leftrightarrow |-1/2\rangle$ transition was not detected because at low fields the transition frequency fell into the region limited by laser-frequency fluctuations, and at higher fields the signal was too weak to detect.

Analysis of the enhanced nuclear Zeeman tensor γ^{Pr} has previously been made in low magnetic fields ($B = 100$ G).[6] Our work extends the analysis to higher values of B where the enhanced Zeeman interaction becomes comparable to the pseudoquadrupole interaction. Taking Reddy and Erickson's values[6] for the γ^{Pr} tensor as a starting point we fit our data to a numerically diagonalized Hamiltonian. The orientation of **B** with respect to the crystal axes and the values of γ_z^{Pr} and γ_x^{Pr} were used as adjustable parameters in fitting the data. We determined (adopting the convention that $E > 0$), that the x axis of the quadrupole tensor must be chosen along the crystal C_2 symmetry axis, which is opposite to Reddy and Erickson's choice of x and y axes for the gyromagnetic tensor, γ^{Pr}. Figure 8 displays the rf data and the numerical fit for an orientation of **B** of $\theta = 1.5°$ and perpendicular to the C_3 axis. The parameter θ is the angle between the applied magnetic field **B** and the local quadrupole x axis (a C_2 axis). For this measurement, the laser electric field $\mathbf{E}_L$ was approximately parallel to **B**. While our fit is insensitive to the value of γ_y^{Pr}, we use a value[6] of $\gamma_y^{Pr}/2\pi = 4.98$ kHz and obtain

$$\gamma_z^{Pr}/2\pi = 10.16 \pm 0.05 \text{ kHz/G}$$

and

$$\gamma_x^{Pr}/2\pi = 3.45 \pm 0.05 \text{ kHz/G} .$$

The sign and value of γ_x^{Pr} is not sensitive to the fit of the data in the linear Zeeman region. Our data in the sensitive nonlinear Zeeman region dictated our choice of γ_x^{Pr}.

V. THE LEVEL REPULSION EFFECT

Of particular interest in carrying out spectroscopy by use of transient rf optical method is the effect of level repulsion that is observed in the region of Pr-F cross relaxation. In Sec. IV the rf data are fitted to the Pr-spin Hamiltonian of Eq. (1) and ignores the relatively weaker magnetic dipole-dipole interaction with the abundant nuclei. Since the dipole-dipole interaction decreases rapidly with distance, in the next approximation one may consider an isolated Pr spin together with the nearest-neighboring nuclei as an isolated system and calculate its energy levels in the presence of an applied magnetic field. In reality, the Pr-F pair interaction is not isolated from the bulk F nuclei and therefore it is broadened by the dipolar coupling among the abundant F spins. The dipole-dipole interaction of the isolated Pr spins with the neighboring fluorine spins results in the broadening of Pr-spin resonances, but in most instances no structure can be seen. The situation is different when at certain values of the external magnetic field the fluorine NMR line matches one of the Pr hyperfine transitions. Figure 9(a) shows a Pr hyperfine energy-level diagram (solid line) together with the fluorine-spin Zeeman energy levels (dashed line), in an approximation where the coupling

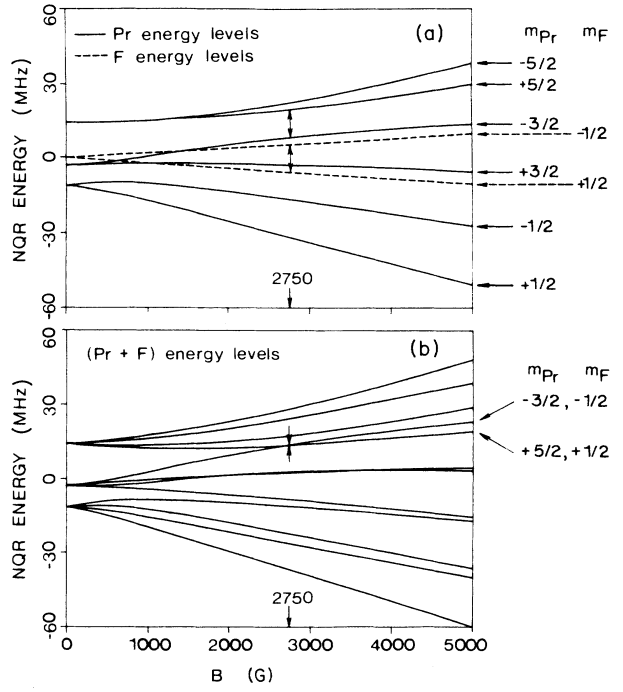

FIG. 9. The Pr-F level crossing for $\theta = 1.5°$. (a) Energy levels of isolated Pr (solid line) and F (dashed line) spins. The cross relaxation at $B = 2750$ G is a result of the matching of the Pr $|+\frac{5}{2}\rangle \leftrightarrow |-\frac{3}{2}\rangle$ and F $|+\frac{1}{2}\leftrightarrow|-\frac{1}{2}\rangle$ transitions. (b) Energy levels of the coupled Pr-F spin system. When Pr and F spins are treated together as one system, the matchings of Pr and F transition frequencies are interpreted as anticrossings of the combined $|+\frac{5}{2},+\frac{1}{2}\rangle$ and $|-\frac{3}{2},-\frac{1}{2}\rangle$ energy levels.

among the spins is ignored. (The orientation of the external magnetic field is perpendicular to the C_3 crystal axis and at $\theta = 1.5°$ with respect to the quadrupole x axis.) A particular Pr-F nuclear transitions crossing is shown at $B = 2750$ G where the fluorine NMR line matches the Pr $(+\frac{5}{2}\leftrightarrow-\frac{3}{2})$ line. This situation resembles the case of two neighboring protons in gypsum,[8] discussed in the Introduction. Although the proton resonances are broadened by the interaction with the more remote nuclei, strong dipolar coupling between the two nearby identical spins results in a Pake doublet, but actually the Pr-F coupling is more complex due to the many F spins forming the group.

In order to obtain an approximate understanding of the Pr^{3+} eigenlevel spectrum in the region where energy conserving flip of a Pr spin and a simultaneous flop of only one of the neighboring F spins occur, we consider only the simpler system with a single Pr spin coupled to a single F spin. The corresponding Hamiltonian is

$$\mathcal{H} = \mathcal{H}_{Pr} + \gamma_F \mathbf{B}\cdot\mathbf{S} + A[I_Z^{Pr}S_z^F - \tfrac{1}{4}(I_+^{Pr}S_-^F + I_-^{Pr}S_+^F)] , \quad (11)$$

where $\mathcal{H}_{Pr}$ is the Pr^{3+} Hamiltonian [Eq. (1)], the second term represents the F-spin Zeeman energy, and A measures the strength of the dipolar coupling between the spins. We ignore the nonsecular terms. The energy-level diagram of this system, obtained by numerical diagonalization of the Hamiltonian in Eq. (11), is shown in Fig. 9(b). When Pr and F spins are treated together as one system, the matchings of Pr and F transition frequencies appear as level crossings of the combined $|m_{Pr},m_F\rangle$ eigenlevels. In particular, the matching of the Pr-$(+\frac{5}{2}\leftrightarrow-\frac{3}{2})$ and F-spin Zeeman line at $B = 2750$ G is seen in Fig. 9(b) as the level crossing of the $|+\frac{5}{2},+\frac{1}{2}\rangle$ and $|-\frac{3}{2},-\frac{1}{2}\rangle$ energy level. A portion of the theoretical spectrum in the region of levels anticrossing at $B = 2750$ G is plotted in Fig. 10, together with the experimental measurements. A dipole-dipole coupling of $A = 100$ kHz is assumed because the rf data are only exact enough to determine that the coupling constant is between 50 and 400 kHz. As the F and Pr $(+\frac{5}{2}\leftrightarrow-\frac{3}{2})$ lines approach one another, a slight deflection from the smooth plot of ω versus B on either side of the point where exact level crossing occurs. In the theoretical model this effect can be interpreted as a result of an anticrossing of the mutual Pr-F eigenlevels. The levels are prevented from crossing by the presence of the flip-flop term of the dipole-dipole interaction that couples the two states. Instead, the levels "repel" one another, and wave functions of the two states interchange their identities as the external magnetic field changes through the region of crossing. The discontinuity of the Pr $(+\frac{5}{2}\leftrightarrow-\frac{3}{2})$ line at $B = 2750$ G is therefore a result of the anticrossing of the $|+\frac{5}{2},+\frac{1}{2}\rangle$ and $|-\frac{3}{2},-\frac{1}{2}\rangle$ energy levels. In fact, any Pr line that represents a transition from either of the levels $(+\frac{5}{2})$ or $(-\frac{3}{2})$ should exhibit such a discontinuity. In rough agreement with this model, a splitting of the Pr $(-\frac{5}{2}\leftrightarrow-\frac{3}{2})$ line was observed (see Fig. 10). Also, as expected, no splitting of the Pr $(+\frac{3}{2}\leftrightarrow-\frac{1}{2})$ line was observed since this transition is not connected to any of the paired Pr coupled eigenlevels that cross relax with F spins.

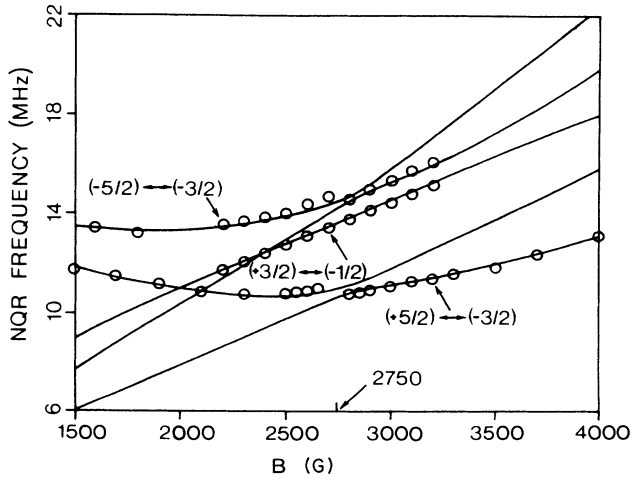

FIG. 10. Observed level repulsion (circles) where the condition for cross relaxation with the fluorine-spin reservoir is satisfied. The numerical fit is obtained by diagonalizing a 12×12 dimensional matrix of the F-Pr^{3+}-coupled Hamiltonian. Only the transitions of interest are shown.

Because our measurement technique relies on sudden rf coupling of the Pr levels and the transient exchange of their populations, no signal from the Pr ($+\frac{5}{2}\leftrightarrow-\frac{3}{2}$) transition is seen at the exact point of level crossing (see Fig. 11). Since the resonant spin flip-flop interaction provides a constant coupling between levels, both levels are bleached by the optical process. Externally applied rf coupling thus has no effect on the laser-beam absorption. This absence of signal at exact resonance provides an additional proof that resonant cross relaxation is taking place.

VI. LEVEL-CROSSING RESULTS

Optical detection of nuclear cross relaxation was also carried out without the use of magnetic resonance. The experimental arrangement (see Fig. 12) was very similar to the rf spectroscopy experiment described above. In the previous experiment, resonant rf pulses were applied to the sample, causing transient perturbations in optical absorption. In this experiment, transient perturbations in optical absorption were induced by sweeping an external magnetic field through resonant values of B where cross relaxation between Pr spins and the fluorine spin reservoir occurs. Light transmission was monitored on a Biomation 8100 transient waveform recorder and averaging performed on up to 75 traces. As the magnetic field changed, both the Pr energy-level splittings and those of the fluorines changed at different rates. During the Zeeman-field sweep several energy matchings occurred which were observed as sharp optical-absorption peaks.

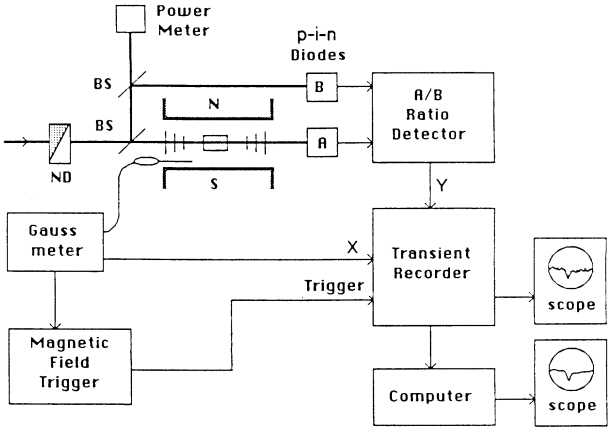

FIG. 12. Experimental apparatus for the level-crossing experiment. The magnetic field is swept rapidly (500 G/sec) and changes in optical absorption noted. BS is the beam splitter; ND is the neutral density wedge.

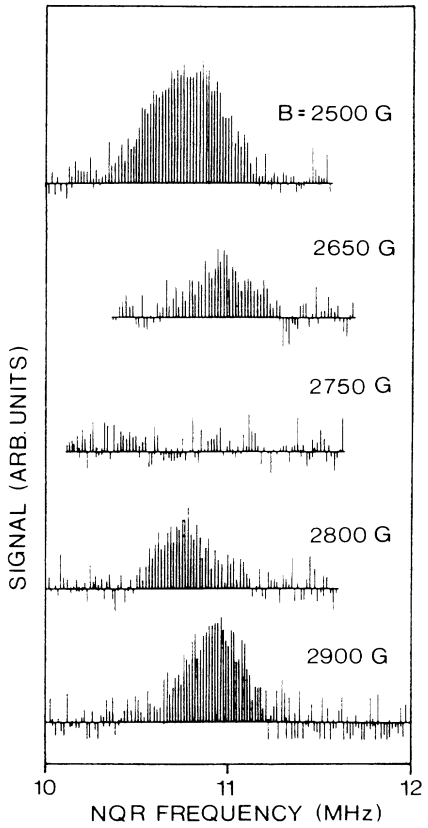

FIG. 11. Temporal rf optical-absorption signals at different external magnetic fields. The nuclear quadropole resonance (NQR) decreases in size as the cross-relaxation resonant value of $B = 2750$ G is approached from either side, and is absent at exact resonance.

According to the theoretical model discussed in Sec. III positions of the absorption peaks can appear shifted from the exact-energy-matching condition (see Fig. 6). The magnitude and direction of the shift depends on the relative rates of optical pumping, magnetic-field B sweep, and cross relaxation. The sign of the shift of the absorption peak changes with the direction of magnetic-field sweep, and therefore sweeps of the magnetic field in both directions produce a symmetrical pair of signals centered at the exact level crossing. Magnetic field sweeps in both directions were employed in order to determine and compensate for errors caused by these shifts.

Figure 13 shows optical transmission during forward and reverse magnetic-field sweeps when the crystal axes were aligned so that the external magnetic field made an angle of 1.5° with respect to a crystal C_2 axis and was perpendicular to the crystal C_3 axis. The laser electric field $\mathbf{E}_L$ was approximately parallel to $\mathbf{B}$. In agreement with the rf spectroscopy results (Fig. 8), absorption peaks were observed for both directions of magnetic-field sweep in the region of the Pr ($+\frac{5}{2}\leftrightarrow-\frac{3}{2}$) and F ($+\frac{1}{2}\leftrightarrow-\frac{1}{2}$) NMR transition matching condition at 2750 G. At the onset of level crossing, a steep drop in laser transmission was followed by a slow recovery beyond the level-crossing condition. This is the result both of the laser frequency width (≈ 1 MHz) and of the slow rate of optical hole burning during the magnetic-field sweep. The large observed linewidth (≈ 150 G) is a consequence of the very small effective gyromagnetic ratio of the Pr ($+\frac{5}{2}\leftrightarrow-\frac{3}{2}$) line in this region. Since observations showed that the error in determining the positions of the

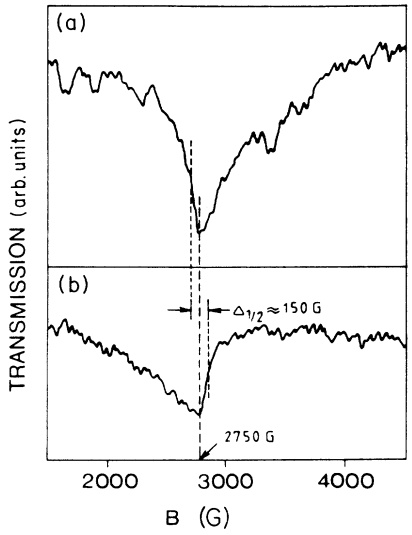

FIG. 13. Optical transmission during increasing (a) and decreasing (b) magnetic-field sweep. Magnetic field B is at an angle of 1.5° with respect to the C_2 axis and is perpendicular to the crystal C_3 axis. Laser light is polarized parallel to B. The absorption peak at $B=2750$ G corresponds to the matching of Pr $|+\frac{5}{2}\rangle \leftrightarrow |-\frac{3}{2}\rangle$ and F $|+\frac{1}{2}\rangle \leftrightarrow |-\frac{1}{2}\rangle$ transition frequencies.

absorption peaks was less than ±25 G in either magnetic-field sweep direction, only forward sweeps were performed in later experiments.

When the crystal C_2 axis is nearly parallel to **B**, the value of magnetic field at points where level crossing occurs is very sensitive to small angular misalignments. By observing the absorption peaks we were able to reorient the crystal so that the **B** field and one of the C_2 axes were misaligned by less than 0.2°. With this crystal orientation a laser field E_L, when polarized perpendicular to **B**, excites only the sites with a quadrupole x axis at an angle of $\theta=60°$ with respect to **B**. When the laser is polarized parallel to **B**, an additional set of sites with quadrupole x axes parallel to **B** ($\theta=0°$) is excited. The eigenlevel diagram for each set of sites is shown in Figs. 14(a) and 14(b). The corresponding level crossing and enhanced absorption is shown in Fig. 14(c). Additionally, rf data for $\theta=60°$ are shown in Fig. 14(a). After the first crossing of a given Pr transition with the fluorine reservoir, the Pr levels are depopulated and subsequent crossings of the same Pr line in a time short compared to spin-lattice relaxation are less effective, and absorption is not observed. Both single and less probable double fluorine spin-flip interactions with Pr spins are observed. Similar measurements were conducted for a different crystal orientation where sites with $\theta=30°$ and $\theta=90°$ were excited. The observed absorption peaks agree well with predictions of the energy-level crossings calculated from the spin Hamiltonian in Eq. (11).

When a cw rf signal of fixed frequency is applied during a magnetic-field sweep, additional absorption peaks, not shown here, were observed. As Pr hyperfine-transition frequencies change with the magnetic field, at certain values of B the frequency of the applied external

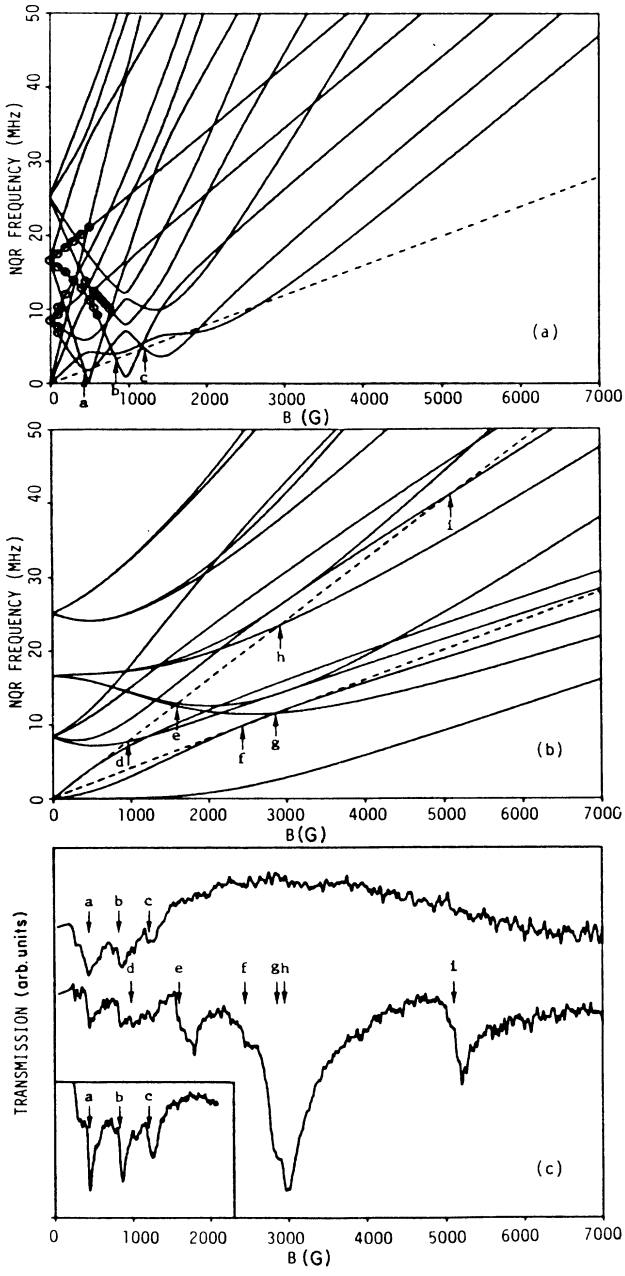

FIG. 14. (a) rf data (circles) and numerical calculation (solid line) for $\theta=60°$, $\gamma_x^{Pr}/2\pi=3.45$ kHz/G, $\gamma_y^{Pr}/2\pi=4.98$ kHz/G, and $\gamma_z^{Pr}/2\pi=10.16$ kHz/G. The dashed line is the fluorine transition. Arrows show where energy-conserving cross relaxation occurs. Note that only the first crossing point of a given Pr^{3+} line is indicated (see text). (b) Same as (a), but with $\theta=0°$. Double fluorine-spin-flip transitions are also shown (upper dashed line). (c) Optical transmission during magnetic-field sweep at a rate of 500 G/sec. The upper curve represents the average of 20 traces, where E_L was perpendicular to B and one of the C_2 axes, exciting only sites with $\theta=60°$. The lower curve represents the average of 75 traces under the same conditions. The middle curve shows optical transmission for the case where E_L was parallel to B and one of the C_2 axes. In this case, sites with $\theta=60°$ and $\theta=0°$ were excited simultaneously. Double spin-flip transitions were observed only for $\theta=0°$.

rf matches that of a Pr hyperfine transition. Analogous to the case of Pr-F cross relaxation, this causes a rapid change of population differences between Pr hyperfine levels and a transient change in the optical pumping process. By shifting the rf frequency between each magnetic-field sweep, NMR spectroscopy of the hyperfine levels can thus be mapped out, which we did not carry out in detail. This magnetic-field sweep combined with rf saturation provides an additional method for carrying out optical spectroscopy.

VII. DYNAMIC-SPIN-RESERVOIR POLARIZATION

Optical pumping has been demonstrated to be a useful technique for achieving nuclear polarization in solids.[16–18] We now discuss the prospects for obtaining a net polarization of fluorine spins exceeding the Boltzman equilibrium by means of cross relaxation of the fluorine spins with the optically pumped Pr^{3+} system. As noted in Sec. III and stated explicitly in the Appendix, the cross relaxation between fluorine spins and optically pumped Pr^{3+} spins does not change the net fluorine-spin-reservoir polarization. This concerns the Pr-spin cross-coupled-ground-state levels α and β ($E_\beta > E_\alpha$). The symmetry of the combined optical-pumping–cross-relaxation process produces two polarized Pr-spin groups A and B with equal but opposite polarizations [$p(A) = -p(B)$]. The Pr-spin polarization for each of the groups is defined by $p = (n_\alpha - n_\beta)/(n_\alpha + n_\beta)$. This leads to the local cooling or heating of the fluorine spins but the fluorine spin temperature averaged over the sample does not change. As a result of the optical pumping combined with cross relaxation, the rate at which Pr spins polarize the neighboring fluorines under steady-state conditions is very slow. The two coupled α and β Pr levels are bleached and therefore the effective number of Pr spins that can exchange energy with the surrounding fluorines becomes rather small.

In order to produce a nonzero net polarization of the fluorine spins a reduction in symmetry of the optical pumping cycle of the Pr^{3+} ions is required. This can be accomplished by connecting either (but not both) of the levels α or β with at least one of the four levels σ by means of rf saturation, with the result that $p(A) \neq -p(B)$ and $p(C) \neq 0$. The largest effect on the Pr-spin polarization is obtained when all four σ levels are coupled to either one of the α or β levels. If any of the NMR transitions is forbidden, the coupling can be achieved by two photon transitions. An additional effect of the induced rf NMR saturations is that the bleaching of levels α or β is hindered by the increased rate of repopulation from levels σ. As a result, the number of Pr spins in levels α and β increases, making the cross relaxation more effective.

In the following analysis we consider a case when the rf NMR transitions couple all σ levels to level β (see Fig. 15). The situation where σ levels are coupled to level α is analogous and results in equal but opposite Pr-spin- and F-spin-reservoir polarizations. The ratio ϵ of the number of all optically excited Pr^{3+} ions to the total number of fluorines in Pr^{3+}:LaF_3 is very small. The Pr^{3+} ions replace approximately 10^{-2} La^{3+} ions, and only 10^{-4} Pr^{3+} ions are in resonance with the narrow-linewidth laser. Therefore $\epsilon \approx 10^{-6}$, and if the cross relaxation is not diffusion limited, we can assume that the polarization of the large fluorine spin system does not change appreciably in the time needed for the Pr-spin-group level populations to reach quasiequilibrium after the onset of level crossing. In this adiabatic approximation the Pr-spin-level populations of groups A, B, and C can be calculated using rate equations similar to the rate Eqs. (3), where the coupling between levels α and β due to the Pr-F cross relaxation is described by a rate W_C. In writing rate equations we use the same notation for the rates but slightly different notation for the level populations as compared to the notation in Sec. III. The effect of the induced NMR transitions between level β and levels σ is described by a rate $W_{\rm rf}$ ($\sec^{-1}$). The populations of levels α and β of Pr-spin groups are represented by n_α and n_β, respectively. For the analysis in this section the excited optical state populations are described by n_ξ. The combined population of the four σ levels of groups A and B is represented by n_σ. The level populations of all three groups A, B, and C are normalized to one separately. The rate equations describing the combined effect of the cross relaxation and the induced NMR transitions on the optical pumping cycle of the Pr^{3+} ions in group A are, therefore,

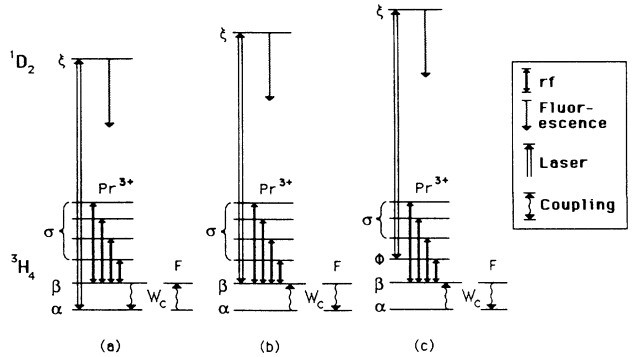

FIG. 15. The proposed scheme for achieving fluorine-spin polarization. Inhomogeneous broadening allows the pumping cycles shown in (a), (b), and (c) to occur simultaneously.

$$\frac{dn_\alpha}{dt} = W_L(n_\xi - n_\alpha) + W_C(n_\beta - n_\alpha) + \frac{n_\xi}{6T_f} + W_{\rm sl}[(n_\beta + n_\sigma) - 5n_\alpha] , \tag{12a}$$

$$\frac{dn_\beta}{dt} = W_C(n_\alpha - n_\beta) + \frac{n_\xi}{6T_f} + W_{\rm sl}[(n_\alpha + n_\sigma) - 5n_\beta] + W_{\rm rf}(n_\sigma - 4n_\beta) , \tag{12b}$$

$$\frac{dn_\sigma}{dt} = \frac{4n_\xi}{6T_f} + W_{\rm sl}[4(n_\alpha + n_\beta) - 2n_\sigma] + W_{\rm rf}(4n_\beta - n_\sigma) , \tag{12c}$$

$$\frac{dn_\xi}{dt} = W_L(n_\alpha - n_\xi) - \frac{n_\xi}{T_f} , \tag{12d}$$

and

$$\sum_i n_i \equiv 1 \ , \tag{12e}$$

where $i=\alpha$, β, σ, and ξ. The rate equations for the Pr^{3+} ions in the group B are given by

$$\frac{dn_\alpha}{dt} = W_C(n_\beta - n_\alpha) + \frac{n_\xi}{6T_f} + W_{sl}[(n_\beta + n_\sigma) - 5n_\alpha] \ , \tag{13a}$$

$$\frac{dn_\beta}{dt} = W_L(n_\xi - n_\beta) + W_C(n_\alpha - n_\beta) + \frac{n_\xi}{6T_f} + W_{sl}[(n_\alpha + n_\sigma) - 5n_\beta] + W_{RF}(n_\sigma - 4n_\beta) \ , \tag{13b}$$

$$\frac{dn_\sigma}{dt} = \frac{4n_\xi}{6T_f} + W_{sl}[4(n_\beta + n_\alpha) - 2n_\sigma] + W_{rf}(4n_\beta - n_\sigma) \ , \tag{13c}$$

$$\frac{dn_\xi}{dt} = W_L(n_\beta - n_\xi) - \frac{n_\xi}{T_f} \ , \tag{13d}$$

and

$$\sum_i n_i \equiv 1 \ . \tag{13e}$$

In order to describe the optical pumping–cross-relaxation process of the Pr^{3+} ions in group C, we use the following notation. Population n_ϕ represents that σ level which is in resonance with the laser excitation, while the population n_σ represents the remaining three σ levels [see Fig. 15(c)]. The rate equations for the group C are therefore

$$\frac{dn_\alpha}{dt} = W_C(n_\beta - n_\alpha) + \frac{n_\xi}{6T_f} + W_{sl}[(n_\beta + n_\sigma + n_\phi) - 5n_\alpha] \ , \tag{14a}$$

$$\frac{dn_\beta}{dt} = W_C(n_\alpha - n_\beta) + \frac{n_\xi}{6T_f} + W_{sl}[(n_\alpha + n_\sigma + n_\phi) - 5n_\beta] + W_{rf}(n_\sigma + n_\phi - 4n_\beta) \ , \tag{14b}$$

$$\frac{dn_\sigma}{dt} = \frac{3n_\xi}{6T_f} - W_{sl}[3(n_\alpha + n_\beta + n_\phi) - 3n_\sigma] + W_{rf}[3(n_\beta + n_\phi) - 2n_\sigma] \ , \tag{14c}$$

$$\frac{dn_\phi}{dt} = W_L(n_\xi - n_\phi) + \frac{n_\xi}{6T_f} + W_{sl}[(n_\alpha + n_\beta + n_\sigma) - 5n_\phi] + W_{rf}(n_\beta + n_\sigma - 4n_\phi) \ , \tag{14d}$$

$$\frac{dn_\xi}{dt} = W_L(n_\phi - n_\xi) - \frac{n_\xi}{T_f} \ , \tag{14e}$$

and

$$\sum_i n_i \equiv 1 \ . \tag{14f}$$

We assign to the optically excited Pr spins an average polarization p', defined by

$$p' = \frac{(n_A + n_B + 4n_C)}{(n_{0A} + n_{0B} + 4n_{0C})} \ . \tag{15}$$

Here n_j and n_{0j} (where $j = A$, B, and C) represent the difference $n_j = n_{\alpha j} - n_{\beta j}$ and the sum $n_{0j} = n_{\alpha j} + n_{\beta j}$, respectively of the levels α and β of each of the groups A, B, and C. In Eq. (15) we took into account that the group C has a weight of four. We assume that the external magnetic field is fixed at or near a Pr-F–spin-level crossing. Assuming an infinite lattice temperature, the average fluorine spin reservoir polarization P', defined by

$$P' = \frac{n_\alpha(\mathrm{F}) - n_\beta(\mathrm{F})}{n_\alpha(\mathrm{F}) + n_\beta(\mathrm{F})} \ , \tag{16}$$

can be described by

$$\frac{dP'}{dt} = 2r\epsilon W_C(p' - P') - \frac{P'}{T_{1F}} \ , \tag{17}$$

and T_{1F} represents the fluorine-spin-lattice relaxation time. In Eq. (16), n_α(F) and n_β(F) pertain to the total F-spin reservoir populations of the lower and upper Zeeman energy levels, respectively. The factor $r = (n_{0A} + n_{0B} + 4n_{0C})/6$ represents the ratio of the number of Pr spins in levels α and β to the total number of Pr spins, where only spins belonging to groups A, B, or C are taken into account. In this simplified model the Pr spins reach a quasiequilibrium average polarization p'_{eq} in a time determined by the slowest of the rates $W_{sl} = 10^{-1}$ sec^{-1}. The "slow" fluorine-spin reservoir then couples with the quasi-steady-state Pr-spin polarization p'_{eq}. For times $t \ll [(\epsilon W_C)^{-1}, T_{1F}]$, Eq. (17) can be approximated by

$$\frac{dP'}{dt} \approx 2r\epsilon W_C p'_{eq} \ . \tag{18}$$

The cross-relaxation rate W_C is adjustable by the external magnetic field by means of the level-crossing tuning parameter [see Eq. (4)]. In order to apply the rapid-spin-diffusion limit ($W_c < 10^4$ sec^{-1}) we set $W_c = 10^2$ sec^{-1}. For a typical laser-excitation rate $W_L = 10^3$ sec^{-1} and the external rf NMR excitation rate $W_{rf} = 10^3$ sec^{-1}, with $T_f = 5 \times 10^{-4}$ sec, the steady-state solutions to rate Eqs. (12), (13), and (14) result in an average Pr quasiequilibrium polarization of 20% ($p'_{eq} = 0.2$) with a correction factor $r = 0.4$. Equation (18) then predicts that for these parameters a net F-spin reservoir polarization of 1% ($P' = .01$) can be achieved in about 1000 sec if T_{1F} is that long or longer. The sign of the imposed fluorine-spin reservoir polarization depends on which of the two Pr-spin levels α or β is chosen to be connected by the external rf NMR transitions to the remaining four σ levels.

VIII. CONCLUSION

Measurements of optical transmission during the magnetic-field sweep have been made in order to detect interspecies nuclear spin-spin reservoir cross relaxation in Pr^{3+}:LaF_3, where the Pr spins couple to the surrounding

F-spin reservoir by level crossing controlled by means of the Zeeman field. Several couplings between different $^3H_4$ ground states of Pr with F spins are observed. The optical pumping is combined with a magnetic field sweep method which causes cross relaxation between two spin species. This procedure is useful for checking a few regions in rather complicated types of Breit-Rabi hyperfine level diagrams without the necessity of carrying out rf resonance signal detection.

Transient optical spectroscopy by use of NMR proved to be a reliable means of mapping more completely the Pr^{3+} ground-state hyperfine-spin-level spectrum over a wide range of Zeeman magnetic fields. A level repulsion effect in the Pr^{3+}:LaF_3 NMR spectrum was observed in the region of Pr-F spin-spin reservoir cross relaxation, and was interpreted as an anticrossing in the combined Pr+F energy-level diagram. The size of the level repulsion indicates a coupling of about $|\Delta\nu|=200$ kHz, in agreement with the inhomogeneous broadening of ≈ 100 kHz due to the static magnetic fields of the surrounding fluorine nuclei.

No crossings with lanthanum quadrupole levels were identified. This can be explained by the fact that the La concentration is one third that of the F-spin concentration, and also because the shortest interatomic distance between La and Pr spins is twice that between Pr and F spins.[14] Transition probabilities for cross-relaxation between Pr and La are expected to be weak because both systems are made up of mixed states in the presence of a B field.[19]

From a set of detailed balance rate equations which express the two reservoir spin-spin coupling rate between F and Pr systems, together with rf saturation transitions, we show theoretically that a substantial equilibrium net polarization of F spins might be achieved by means of optical pumping. This technique may be advantageous in cases where a quick recovery of spin population is required for NMR studies which would otherwise be impractical because of a long T_1.

ACKNOWLEDGMENTS

This work was supported by the National Science Foundation. One of us (M.L.) acknowledges the support of the Center for Electrooptics, Ljubljana, Yugoslavia.

APPENDIX

In the diffusion-limited case for Pr-F spin coupling we improve upon a model[9] which is based upon the assumption of a spherically symmetric continuum of F-spin density surrounding each isolated Pr spin. In order to apply the concept of isotropic spin diffusion we assume that the F spins in a volume $4\pi r_0^3/3$ are directly dipolar coupled to single Pr spins only over a radius r_0. Beyond this radius which is somewhat arbitrary, the spin coupling rate $1/T_2$(F-F) is dominant among the spins in the fluorine reservoir. If we define a measured[20] bandwidth for the F-F interaction in LaF_3 as $\delta\omega\approx(\hbar\gamma_F^2/r_{FF}^3)=10$ kHz, then r_0 needs to be greater than the radius of the frozen core $r_1=(\gamma_{Pr}\gamma_F/\delta\omega)^{1/3}$. For estimated values of γ_{Pr} less than 4 kHz/G extending to about 7 kHz/G, the radius r_1 extends correspondingly from less than the average distance $d=2.6$ Å between a Pr spin and the first shell of F neighbors to a distance just beyond d. Crudely speaking, this distance d defines the outermost radius of the frozen core of the F spins, beyond which spin diffusion of the F spins at r_1 is the only coupling mechanism to the F-spin reservoir in the region $r>r_1$. Therefore we must add an extra rate equation to those equations listed as Eq. (3) for the rate of change of the average F-spin polarization probability P_0 in the volume $\Delta V=4\pi r_0^3/3$ as

$$\frac{\partial P_0}{\partial t}=\eta W(p-P_0)+\frac{3}{r_0}D\left[\frac{\partial P}{\partial r}\right]_{r_0}. \tag{A1}$$

The first term on the right side of Eq. (A1) represents the driving Pr-F dipolar coupling due to optically pumped Pr spins, valid for either the A or B group. With the use of Fick's law for spin diffusion from a surface of $4\pi r_0^2$, the diffusion term in Eq. (A1) expresses the average spin-density-diffusion rate out of the volume ΔV at radius r_0. The probabilities of Pr- and F-spin polarizations are defined, respectively, by

$$p=\frac{n_\alpha-n_\beta}{N_{Pr}}, \tag{A2}$$

and

$$P=\frac{n_\alpha(\mathrm{F})-n_\beta(\mathrm{F})}{N_F}, \tag{A3}$$

where $N_{Pr}=(n_\alpha+n_\beta)$, $N_F=N_\alpha(\mathrm{F})+n_\beta(\mathrm{F})$, and $\eta=N_{Pr}/N_F$. In the average fluorine polarization probability P_0 over the volume ΔV, N_F pertains to the total number of F spins contained in ΔV multiplied by the number of optically excited Pr ions in either group A or B. For Pr spins from group C, levels α and β are equally populated [$p(C)=0$] and therefore they have no effect on the fluorine reservoir. Because of the optical pumping of n_α or n_β states, the quantity N_{Pr}, defined for each of the groups A or B separately, is time dependent, decreasing with time during the onset of $n_\alpha\rightarrow n_\beta$ transitions. We make the assumptions that $p(t)$ and $\eta(t)$ in Eq. (1A) remain valid in spite of the fact that N_{Pr} is time dependent. In the presence of these nonlinearities the Pr-F systems evolve toward a final spin temperature during the time they are in contact. The radius r_0 defines a mean distance at which direct Pr-F dipolar coupling falls off to a value such that $\partial P/\partial t$ depends mainly on $(\partial P/\partial r)_{r_0}$. Depending on how W changes as resonance is approached in our technique, both r_0 and $(\partial P/\partial r)_{r_0}$ have a slow time dependence. In our approximate model we assign r_0 a constant time averaged value. The F-spin diffusion constant D in Eq. (A1) is approximated by[21]

$$D\approx\frac{a^2}{10}(\langle\Delta\omega_{FF}^2\rangle)^{1/2}, \tag{A4}$$

where a is the internuclear spacing. We realize that the application of an isotropic spin diffusion coefficient D presumes a continuum of spin density. However, in reali-

ty an isolated rare spin communicates its polarization to a finite set of nearest-neighboring foreign spins at a finite lattice distance. This problem poses the question of whether or not a spin-diffusion bottleneck can be analyzed using the continuum-diffusion model,[21] but we apply the model, nevertheless.

The diffusion-limited case requires that the statistically independent rate $W_C(n_1-n_2)$ in Eq. (3) be replaced by

$$\frac{\partial p}{\partial t}=W(P-p) , \tag{A5}$$

where $W=2W_C$. The mechanism of Pr-F cross relaxation is now to be considered, and its connection with F-F spin diffusion will be discussed. The rate W may be written as[9]

$$W=\langle \Delta\omega^2\rangle_{\text{Pr-F}}\tau_C g(\omega) , \tag{A6}$$

where

$$\langle \Delta\omega^2\rangle_{\text{Pr-F}}=\frac{2\pi}{\hbar^2}|M|^2\sum_i |B_i|^2 , \tag{A7}$$

with the definitions

$$|M|^2=|\langle E_{\text{Pr}},E_{\text{F}}|I_+^{\text{Pr}}S_-^{\text{Fi}}+I_-^{\text{Pr}}S_+^{\text{Fi}}|E_{\text{pr}}\pm\hbar\omega_{\text{Pr}},E_F\mp\hbar\omega_{\text{F}}\rangle|^2,$$

and

$$B_i=-\tfrac{1}{4}\frac{\gamma_{\text{Pr}}\gamma_{\text{F}}\hbar^2}{r_i^3}(1-3\cos^2\vartheta_i) .$$

The above sum is taken over the neighboring fluorine spin sites within the radius r_0 where r_i and ϑ_i are the polar coordinates of the ith fluorine spin relative to the Pr spin. The energies of the initial and final states must match, and $g(\omega)$ is an overlap function for the resonances. The expression for W in Eq. (A6) is identical with the rate determined by cross relaxation as it occurs in double resonance,[9,10] where in this case the two spin species are both coupled in the laboratory frame. The pair interaction between Pr and F spins is interrupted by the F-F dipolar interactions, expressed by the correlation time $\tau_C\approx\langle\Delta\omega_{\text{FF}}^2\rangle^{-1/2}$, where $\langle\Delta\omega_{\text{FF}}^2\rangle$ expresses the effect of the dipolar coupling among F spins. We assume that the coupling between Pr spins[15] is negligible. If a Gaussian shape is assumed for either resonance then the level crossing tuning parameter can be expressed as

$$g(\omega)=\exp\left[-\frac{(\omega_{\text{Pr}}-\omega_{\text{F}})^2}{2\langle\Delta\omega^2\rangle}\right] . \tag{A8}$$

The F nuclei at distances $r>r_0$ become disordered at a rate

$$\frac{\partial P(r,t)}{\partial t}=D\nabla^2P(r,t) . \tag{A9}$$

In the absence of cross relaxation, the optical pumping produces a polarization of the Pr^{3+} spin groups A and B represented by the net nonzero population differences $p(A)<0$ and $p(B)>0$ where $P(A)=-p(B)$ by symmetry in the high-temperature approximation. In order to analyze the effect of spin diffusion we assume that Pr spins from groups A and B alternately occupy sites in a regular array with a lattice distance r_{AB} which is the average distance between A and B spins. We ignore the Pr spins belonging to group C since they do not affect the overall spin polarization. After the onset of level crossing, group A produces local cooling $[dP_0(A)/dt<0]$ and group B produces local heating $[dP_0(B)/dt>0]$ of the fluorine spins, but the F-spin temperature averaged over the entire sample does not change. Therefore we can assume that $P(r=r_{AB}/2)=0$. This situation is different from the usual double-resonance experiments[9,10] where rare nuclei can be assigned a uniform temperature and the average temperature of the abundant nuclei is consequently altered. If we also assume that $P(r=r_0)=P_0$ then the steady-state solution to Eq. (9A) becomes

$$P(r)=P_0\left[\frac{R}{r}-\frac{2R}{r_{AB}}\right] , \tag{A10}$$

where $R=(r_0r_{AB})/(r_{AB}-2r_0)$. The steady-state solution to Eq. (A1) then gives

$$P_0=\frac{\eta W}{\eta W+3Dr/r_0^3}p . \tag{A11}$$

In the case when

$$3DR/r_0^3\gg\eta W , \tag{A12}$$

spin diffusion among F nuclei is sufficiently rapid to maintain a spatially uniform spin temperature for F nuclei, and there is no diffusion bottleneck for transfer of disorder between Pr and F nuclei. However, a diffusion bottleneck is expected when

$$\eta W\gg 3DR/r_0^3 , \tag{A13}$$

since F nuclei near the Pr nuclei disorder more rapidly than more distant nuclei. The Pr-spin polarizations p and the ratios η are not independent of the fluorine-spin polarizations and in general cannot be calculated separately. However, in the case when the cross coupling is not diffusion limited, $P_0=0$ for all times and Eq. (A5) simplifies to

$$\frac{\partial p}{\partial t}=-Wp , \tag{A14}$$

and the Pr level populations of groups A and B can be calculated separately using Eqs. (3), where the Pr-F cross relaxation is described by a single rate $W_c=W/2$.

Strictly speaking the above conditions [Eqs. (A12) and (A13)] for the spin diffusion are valid only at equilibrium. However, we can assume that the ability of the neighboring fluorine spins at $r>r_0$ to maintain the fluorine spins inside r_0 at the fluorine reservoir temperature diminishes with time as the disorder builds up outside the volume V. We therefore assume that the steady-state conditions [Eqs. (A12) and (A13)], with η substituted for its largest possible value, are valid also for times before the systems reach equilibrium. Before the Pr and F spin systems reach equilibrium the probabilities N_{Pr} and therefore the ratios η vary in time. The largest value for N_{Pr}, of

$N_{Pr}=\frac{1}{3}$, occurs in the absence of optical pumping. The radius r_0 is expected to be of the order of a few lattice parameters, and therefore $N_F \approx 40$. For a 0.5 at. % doped sample of Pr^{3+}:LaF_3, the cross relaxation of a single Pr spin with neighboring F spins can be considered independent from other Pr spins since the average distance r_{AB} is very large, on the order of 100 nm, making $R \approx r_0$. From Eq. (A4) we obtain $D=4\times10^{-16}$ m^2. From the condition in Eq. (A13) it then follows that the cross coupling is diffusion limited for $W \geq 10^4$ sec^{-1}.

In order to estimate W from Eq. (A6) when $\omega_{Pr}=\omega_F$ we use the following values: $\gamma_{Pr}/(2\pi)\approx4$ kHz/G, $\gamma_F/(2\pi)=4$ kHz/G; and $\tau_C=17$ μ sec.[20] By summing the contributions of forty nearest fluorine neighbors (ignoring the angular dependence) we obtain $W \approx |M|^2\times10^6$ sec^{-1}.

Experimentally the evidence in our model for spin-diffusion-limited transfer of spin population between two different spin species can only be confirmed by comparing changes in spin population differences to the prediction of the model. The model reveals a rate transient more complex than W_c. A further investigation of the nonlinear transient solutions to Eq. (A5) would be necessary. Further refinement would require that nonequilibrium initial conditions be well defined which is not the case in our investigation, nor does our method provide a direct determination of changes in spin magnetization which would be achieved by direct NMR measurements.

[1]L. E. Erickson, Phys. Rev. B **16**, (1977) 4731.
[2]R. M. Macfarlane, R. M. Shelby, and R. L. Shoemaker, Phys. Rev. Lett. **43**, 1726 (1979).
[3]N. C. Wong, E. S. Kintzer, J. Mylnek, R. G. DeVoe, and R. G. Brewer, Phys. Rev. B **28**, 4993 (1983).
[4]Y. C. Chen, K. Chiang, and S. R. Hartman, Phys. Rev. B **21**, 40 (1980).
[5]F. W. Otto, M. Lukac, and E. L. Hahn, J. Lumin. **35**, 321 (1986).
[6]B. R. Reddy and L. E. Erickson, Phys. Rev. B **27**, 5217 (1983).
[7]A. Wokaun, S. C. Rand, R. G. DeVoe, and R. G. Brewer, Phys. Rev. B **23**, 5733 (1981).
[8]G. E. Pake, J. Chem. Phys. **16**, 327 (1948).
[9]R. E. Slusher and E. L. Hahn, Phys. Rev. **166**, 332 (1986).
[10]S. R. Hartmann and E. L. Hahn, Phys. Rev. **128**, 2042 (1962).
[11]G. Kothandarman, P. F. Brode III, and D. W. Pratt, Chem. Phys. Lett. **51**, 137 (1977).
[12]L. E. Erickson, Phys. Rev. B **11**, 77 (1975).
[13]M. A. Teplov, Zh. Eksp. Teor. Fiz. **53**, 1510 (1968) [Sov. Phys—JETP **26**, 872 (1968)]; R. Bleaney, Physica **69**, 317 (1973).
[14]A. Zalkin, D. H. Templeton, and T. E. Hopkins, Inorganic Chem. **5**, 1466 (1966).
[15]R. M. Shelby, R. M. Macfarlane, and C. S. Yannoni, Phys. Rev. B **21**, 5004 (1980).
[16]G. Lampel, Phys. Rev. Lett. **20**, 491 (1986).
[17]V. A. Atsarkin, A. E. Mefeod, and M. I. Rodak, Phys. Lett. **27A**, 57 (1986).
[18]W. B. Grant, L. F. Molenauer, and C. D. Jeffries, Phys. Rev. B **4**, 1428 (1976).
[19]L. O. Anderson and W. G. Proctor, Z. Krist. **127**, 366 (1968); L. O. Andersson and G. Johansson, *ibid.* **127**, 386 (1968).
[20]K. Lee and A. Sher. Phys. Rev. Lett. **14**, 1027 (1965); L. Shen, Phys. Rev. **172**, 259 (1968).
[21]N. Bloembergen, Physica **15**, 386 (1949).